

Effect of discrete breathers on the specific heat of a nonlinear chain

Mohit Singh^{1,*}, Alina Y. Morkina^{2,†}, Elena A. Korznikova^{2,3,‡}, Vladimir I. Dubinko^{4,§}, Dmitry A. Terentiev^{5,¶},
Daxing Xiong^{6,**}, Oleg B. Naimark^{7,††}, Vakhid A. Gani^{8,9,‡‡} and Sergey V. Dmitriev^{3,10,§§}

¹Indian Institute of Technology Kharagpur, Kharagpur 721302, India

²Ufa State Aviation Technical University, Ufa 450008, Russia

³Institute for Metals Superplasticity Problems, Russian Academy of Sciences, Ufa 450001, Russia

⁴NSC Kharkov Institute of Physics and Technology, Kharkov 61108, Ukraine

⁵SCK•CEN, Nuclear Materials Science Institute, Boeretang 200, Mol, 2400, Belgium

⁶Department of Physics, Fuzhou University, Fuzhou 350108, Fujian, China

⁷Institute of Continuous Media Mechanics Ural Branch of RAS, Perm 614013, Russia

⁸Department of Mathematics, National Research Nuclear University

MEPhI (Moscow Engineering Physics Institute), Moscow 115409, Russia

⁹Theory Department, National Research Center Kurchatov Institute,
Institute for Theoretical and Experimental Physics, Moscow 117218, Russia

¹⁰National Research Tomsk State University, Tomsk 634050, Russia

Defect-free crystal lattices can accommodate spatially localized, high amplitude atomic vibrations called either discrete breathers (DBs) or intrinsic localized modes (ILMs). This has been explored by a number of molecular dynamics studies and, in few cases, by the first-principles calculations. A number of experimental measurements of crystal vibrational spectra was performed aiming to prove the existence of DBs in thermal equilibrium at elevated temperature. However, the interpretation of these experimental results is still debated. Direct high-resolution imaging of DBs in crystals is hardly possible due to their nanometer size and short lifetime. An alternative way to substantiate the existence of DBs is to evaluate their impact on the measurable macroscopic properties of crystals and validate such prediction. One of such properties is specific heat. In fact, the measurements of heat capacity was done for alpha-uranium by Manley and co-workers in conditions where the presence of DBs was expected. In the present study, employing a one-dimensional nonlinear lattice with an on-site potential, we analyze the effect of DBs on its specific heat. In the most transparent way, this can be done by monitoring the chain temperature in a non-equilibrium process, at the emergence of modulational instability, with total energy of the chain being conserved. For the on-site potential of hard-type (soft-type) anharmonicity, the instability of $q = \pi$ mode ($q = 0$ mode) results in the appearance of long-living DBs that gradually dissipate their energy and eventually the system approaches thermal equilibrium with spatially uniform and temporally constant temperature. The variation of specific heat at constant volume is evaluated during this relaxation process. It is concluded that DBs affect specific heat of the nonlinear chain and for the case of hard-type (soft-type) anharmonicity they reduce (increase) the specific heat.

PACS numbers: 05.45.Yv, 63.20.-e

Keywords: Crystal lattice, nonlinear chain, modulational instability, discrete breather, intrinsic localized mode, heat capacity, specific heat

I. INTRODUCTION

Discrete breathers (DBs) or intrinsic localized modes (ILMs) are spatially localized, large-amplitude oscillations in a nonlinear defect-free lattice. DBs have been discovered three decades ago by theoreticians in one-dimensional nonlinear lattices [1–3] and their properties have been extensively studied, as summarized in

refs. [4, 5].

There exist a number of physical systems where the existence of DBs has been proven experimentally, among them are macroscopic spring-mass chains and arrays of coupled pendula or magnets [6–8], granular crystals [9–16], micro-mechanical cantilever arrays [17–19], electrical lattices [20–22], nonlinear optical devices [23], Josephson junction arrays [24, 25].

Crystal lattices can also accommodate DBs [26] since discreteness of media and non-linearity are the two prerequisites for their existence, and interatomic interactions are indeed anharmonic. A number of successful experimental studies showed the existence of DBs in crystals by measuring the vibrational spectra. The examples include DBs found in alpha-uranium [27–29], helium [30], NaI [31, 32], graphite [33], and PbSe [34].

Contrary to the stable lattice defects, e.g. dislocations or grain boundaries, a direct experimental observation of DBs in crystals is challenging due to their nanometric

*Electronic address: mohitsingh1997@gmail.com

†Electronic address: alinamorkina@yandex.ru

‡Electronic address: elena.a.korznikova@gmail.com

§Electronic address: vlad@quantumgravityresearch.org

¶Electronic address: dterenty@sckcen.be

**Electronic address: phyxiongdxfzu.edu.cn

††Electronic address: naimark@icmm.ru

‡‡Electronic address: vagani@mephi.ru

§§Electronic address: dmitriev.sergey.v@gmail.com

characteristic dimension and short (e.g. picosecond) lifetime. The concentration of DBs in crystals under thermal equilibrium conditions is relatively low [35]. Due to the relatively high excitation energy, the investigation of DBs properties and their role on material's properties is obscured. That is why computer simulation methods play an important role in helping the study of DB properties in various crystals. Earlier, the existence of DBs in strained graphene and graphane (fully hydrogenated graphene) has been confirmed with the help of *ab initio* simulations [36, 37]. Such first-principle simulations impose high computational demands and at present their application is limited to two-dimensional (2D) structures supporting highly localized DBs that can be analyzed in relatively small computational cells. DBs in 3D crystals are studied by means of classical molecular dynamics (MD) methods. For the first time, this method was successfully applied to the study of gap DBs in alkali halide NaI crystal [38] and this study was continued in refs. [39, 40]. Using molecular dynamics, DBs have been found in monoatomic Morse crystals [41, 42], covalent crystals Si, Ge and diamond [43, 44], pure metals [45–50], ordered alloys [51–54], carbon and hydrocarbon nanomaterials [55–67], boron nitride [68], and proteins [69–72]. Essential limitation of any MD model is the choice of the interatomic potentials which largely determine the reliability of the obtained results [66].

An alternative approach to investigate the role played by DBs is to predict how they could impact or alter macroscopic properties of crystals depending on the ambient temperature [73]. Since DBs are nonlinear vibrational modes, their excitation is expected to be triggered by raising the temperature above a certain threshold value [74]. In several experimental works, the effect of DBs on macroscopic properties of crystals has been discussed, in particular, anomalies in thermal expansion [27] and heat capacity [28] of alpha-uranium were attributed to the excitation of DBs at high temperatures. At the same time, it was shown numerically that DBs are responsible for the transition from ballistic to normal thermal conductivity in a nonlinear chain [75].

Identification of thermally excited DBs in lattices requires application of special procedures [40, 74, 76–81]. DBs, as lattice defects, can be distinguished in lattice during the non-equilibrium processes e.g. by absorbing running phonon waves at the boundaries of heated lattice [75, 82–93]. Here we choose an alternative approach related to modulational instability of particular delocalized modes. Such instabilities lead to energy localization in the form of long-living chaotic DBs and subsequent transition to thermal equilibrium [22, 94–103]. In the course of this transition of a nonlinear chain, the local temperature and the specific heat can be calculated. Here, we demonstrate that the specific heat of the crystal containing DBs is different (smaller for the hard-type anharmonicity and larger for the soft-type anharmonicity) from the one measured under thermal equilibrium. This feature can be used as indicator of the activation of DBs

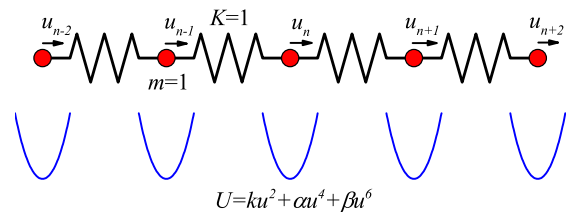


Figure 1: Chain of harmonically coupled, unit mass point-wise particles interacting with the six-order polynomial on-site potential.

while increasing the crystal's temperature and measuring its specific heat at the same time. The specific heat and the anomaly of thermal conductivity in the presence of DBs can be linked also to the definition of the effective temperature related to the additional degrees of freedom of out-of-equilibrium systems.

In this work, we discuss this methodology and provide computational assessment to evaluate the contribution of DBs in the change of the specific heat. After description of the model and simulation procedure provided in Sec. II, the simulation results on the development of modulational instability of the zone boundary mode ($q = \pi$) are presented in Sec. III for the hard-type anharmonicity. The modulational instability of Γ -point mode ($q = 0$) is studied in Sec. IV for the soft-type anharmonicity. Properties of discrete breathers are then analysed in Sec. V to rationalize results of the performed simulations. Summary and conclusions are presented in Sec. VI.

II. THE MODEL AND SIMULATION SETUP

We consider a 1D chain of particles having mass m (see Fig. 1) whose Hamiltonian is defined by

$$H = K + P = \sum_n \frac{m\dot{u}_n^2}{2} + \sum_n \left[\frac{s}{2}(u_{n+1} - u_n)^2 + U(u_n) \right], \quad (1)$$

where K is the kinetic energy, P is the potential energy, u_n is the displacement of the n th particle from its equilibrium position and \dot{u}_n is its velocity (overdot means derivative with respect to time t). The particles are harmonically coupled to their nearest neighbors by the elastic bonds with stiffness s . For the on-site potential, we take

$$U(\xi) = k\xi^2 + \alpha\xi^4 + \beta\xi^6, \quad (2)$$

where k is the coefficient in front of the harmonic term, while the coefficients α and β define the contributions from the quartic and six-order terms, respectively. This model has been considered in [104] for solving a different problem.

Without the loss in generality we set $m=1$, $s = 1$ and for the on-site potential we take $k = 1/2$, $\alpha = \pm 1/24$,

and $\beta = 1/720$. Note that for $\alpha > 0$ we have the on-site potential with the hard-type anharmonicity and for $\alpha < 0$ the on-site potential features the soft-type anharmonicity for not very large vibration amplitudes. On the other hand, for very large vibration amplitudes, when the six-order term dominates, even for $\alpha < 0$, the system demonstrates hard-type anharmonicity, but this case is not addressed here.

The equations of motion that stem from Eqs. (1) and (2) are

$$m\ddot{u}_n = s(u_{n-1} - 2u_n + u_{n+1}) - 2ku_n - 4\alpha u_n^3 - 6\beta u_n^5. \quad (3)$$

These equations are integrated numerically using the Störmer method of order six with the time step $\tau = 10^{-3}$.

In the case of small amplitude vibrations, the nonlinear terms can be neglected and the solutions of the linearized equation are the normal modes $u_n \sim \exp[i(qn - \omega_q t)]$ with wave number q and frequency ω_q . These modes obey the following dispersion relation

$$\omega_q^2 = \frac{2}{m}[k + s(1 - \cos q)]. \quad (4)$$

The considered chain supports the small-amplitude running waves (phonons) with frequencies within the band from $\omega_{\min} = 1$ for $q = 0$ to $\omega_{\max} = \sqrt{5} \approx 2.236$ for $q = \pi$.

In the case of hard-type anharmonicity ($\alpha = 1/24$), the zone-boundary mode with $q = \pi$ and the amplitude A ,

$$u_n = A \sin(\pi n - \omega_{\max} t), \quad (5)$$

is excited in the chain of $N = 1000$ particles at $t = 0$.

For the chain with soft-type anharmonicity ($\alpha = -1/24$) the Γ -point mode with $q = 0$ and the amplitude A ,

$$u_n = A \sin(\omega_{\min} t), \quad (6)$$

is initially excited.

If A is not too small, the above two modes are modulationally unstable. Initially the energy is evenly shared between all the particles. Development of the instability results in energy localization which can be monitored by calculating the localization parameter

$$L = \frac{\sum e_n^2}{\left(\sum e_n\right)^2}, \quad (7)$$

where

$$e_n = \frac{m\dot{u}_n^2}{2} + \frac{s}{4}(u_n - u_{n-1})^2 + \frac{s}{4}(u_{n+1} - u_n)^2 + U(u_n), \quad (8)$$

is the energy of the n th particle.

As a measure of temperature, the averaged kinetic energy per atom,

$$\bar{K} = \frac{1}{N} \sum_n \frac{m\dot{u}_n^2}{2}, \quad (9)$$

will be used. In fact, the temperature of a one-dimensional lattice is $T = 2\bar{K}/k_B$, where $k_B = 8.617 \times 10^{-5} \text{ eVK}^{-1}$ is the Boltzmann constant.

Heat capacity of the whole chain is defined as follows

$$C = \lim_{\Delta T \rightarrow \infty} \frac{\Delta H}{\Delta T}, \quad (10)$$

where ΔH is the portion of energy given to the system and ΔT is the corresponding increase in temperature. Specific heat is defined as the heat capacity per unit mass or per particle. Since periodic boundary conditions are used in this study and thermal expansion of the chain is not allowed, we evaluate the specific heat at constant volume.

The problem with using the definition Eq. (10) is that our simulations are performed at constant total energy H . Hence the specific heat of the chain at constant volume is characterized by the ratio

$$c_V = \frac{\bar{H}}{\bar{K}}, \quad (11)$$

where \bar{H} and \bar{K} are the total energy and the kinetic energy of the chain per atom, respectively.

In linear systems, an increase in the total energy is equally shared between the kinetic and potential energies so that $\bar{H} = 2\bar{K}$ and $c_V = 2$. Whereas in nonlinear systems, the kinetic and potential energies can be different and c_V can deviate from this value.

In the following section, the time evolution of c_V will be calculated for the chain during the development of modulational instability. The values of c_V in the regime when energy is localized by DBs will be compared to that in thermal equilibrium.

III. MODULATIONAL INSTABILITY FOR HARD-TYPE ANHARMONICITY

We take $\alpha = 1/24$ in the on-site potential Eq. (2) and excite the chain in the zone-boundary mode Eq. (5) considering various amplitudes A . While integrating the equations of motion Eq. (3), we monitor the change in the localization parameter L , Eq. (7), and specific heat c_V , Eq. (11).

Localization parameter as a function of time is presented in Fig. 2 for various values of A . At $t = 0$, all curves start from the minimal possible value of the localization parameter that is $L = 1/N = 10^{-3}$. The development of modulational instability results in energy localization due to the formation of DBs and this leads to an increase in the localization parameter. DBs slowly radiate their energy and thus, the localization parameter gradually decreases and in the end, when the system reaches the state of thermal equilibrium, L oscillates near the small value of 2×10^{-3} .

Distribution of energy over the chain at the time when localization parameter is maximal is shown in Fig. 3 for

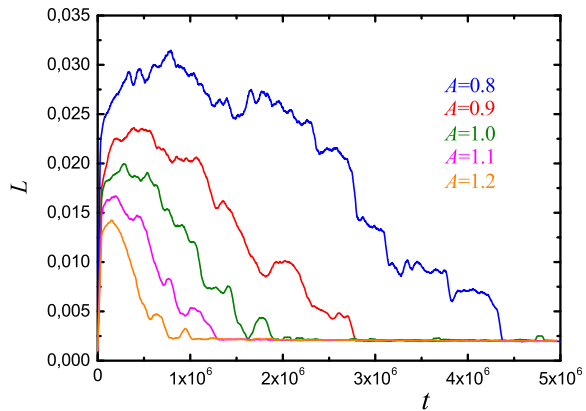


Figure 2: Results of Localization parameter L vs time t ($\alpha = 1/24$, hard-type anharmonicity) for various amplitudes A of the initially excited zone-boundary mode. For all cases at $t = 0$, $L = 1/N = 10^{-3}$. Modulational instability results in increase of L due to energy localization on DBs. Then L decreases because DBs gradually radiate energy and eventually system reaches thermal equilibrium with $L = 2 \times 10^{-3}$.

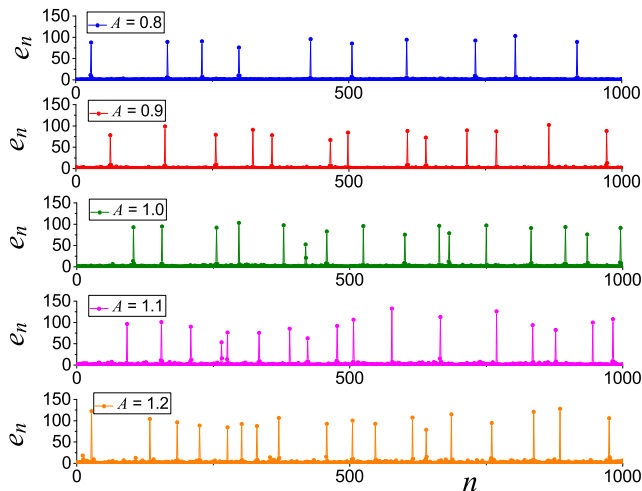


Figure 3: Total energies of particles in the chain at the time when the localization parameter reaches its maximum for various amplitudes of the initially excited zone-boundary mode, as indicated for each panel. Results for $\alpha = 1/24$ (hard-type anharmonicity).

various mode amplitudes from $A = 0.8$ to $A = 1.2$. One can see the sets of DBs sharply localized on single particles. In Fig. 4, we plot (a) the number of DBs and (b) the average energy of DBs as a function of the zone-boundary mode amplitude at the time when L is maximal. It follows from the plots that N_{DB} increases linearly with A nearly two times within the studied range of amplitudes, while E_{DB} increases with A very slowly.

Our main result is shown in Fig. 5, where the time-dependence of specific heat is plotted for the various mode amplitudes. From comparison of Fig. 2 and Fig. 5, it can be seen that the specific heat is minimal when the

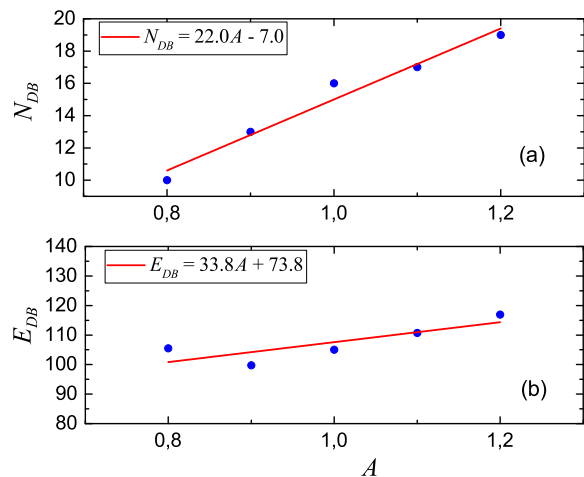


Figure 4: (a) Number of discrete breathers and (b) average energy of discrete breathers at the time when localization parameter is maximal, as the functions of the zone-boundary mode amplitude.

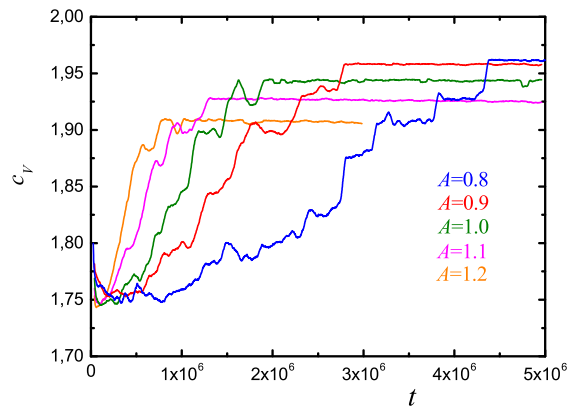


Figure 5: Specific heat normalized by A^2 as the function of time for various amplitudes of the initially excited zone-boundary mode. Inset zooms in the range of small time. Specific heat is minimal when DBs are in the system and it increases while system approaches thermal equilibrium. Results for $\alpha = 1/24$ (hard-type anharmonicity).

localization parameter is maximal. During the transition to thermal equilibrium, the specific heat increases. From this, we conclude that the DBs reduce the specific heat of the chain with hard-type anharmonicity.

IV. MODULATIONAL INSTABILITY FOR SOFT-TYPE ANHARMONICITY

Now, we take $\alpha = -1/24$ in the on-site potential Eq. (2) and excite the chain in the gamma-point mode Eq. (6) considering various amplitudes A . Again, while integrating the equations of motion Eq. (3), we monitor the change in the localization parameter L , Eq. (7), and

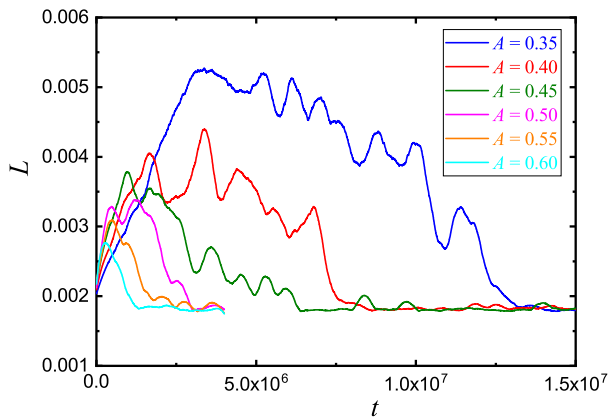


Figure 6: The same as Fig. 2 but for soft-type anharmonicity ($\alpha = -1/24$).

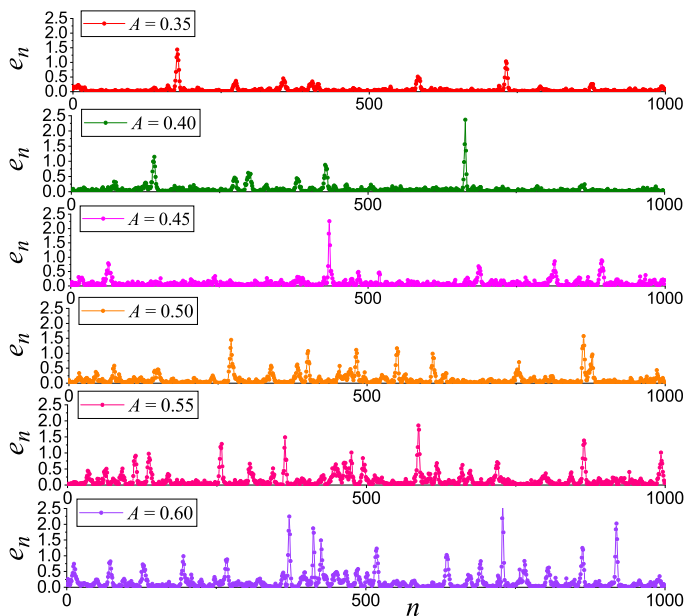


Figure 7: Total energies of particles in the chain at the time when the localization parameter reaches its maximum for various amplitudes of the initially excited gamma-point mode, as indicated for each panel. Results for $\alpha = -1/24$ (soft-type anharmonicity).

specific heat c_V , Eq. (11).

Localization parameter as a function of time is presented in Fig. 6 for various values of A . Similar to the hard-type case, at $t = 0$, all curves start from the minimal possible value of the localization parameter that is $L = 1/N = 10^{-3}$. The development of modulational instability results in energy localization due to the formation of DBs and this leads to an increase in the localization parameter. DBs slowly radiate their energy and thus, the localization parameter gradually decreases and in the end, when the system reaches the state of thermal equilibrium, L oscillates near the small value of 2×10^{-3} .

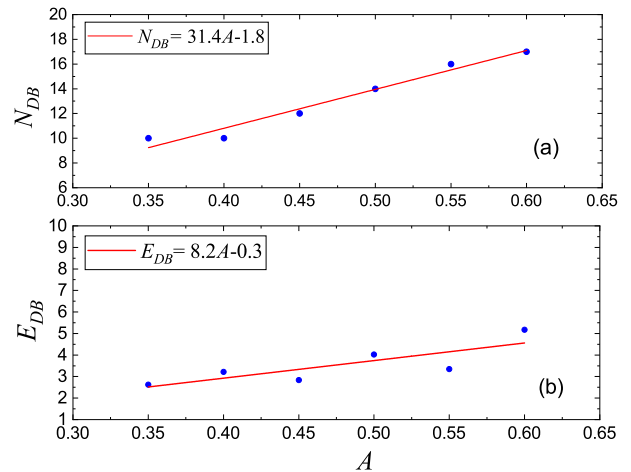


Figure 8: (a) Number of discrete breathers and (b) Average energy of discrete breathers at the time when localization parameter is maximal, as the functions of the gamma-point mode amplitude.

Distribution of energy over the chain at the time when localization parameter is maximal is shown in Fig. 7 for various mode amplitudes from $A = 0.35$ to $A = 0.6$. One can see the sets of DBs sharply localized on single particles (though they are not as sharply localized as in the case of hard-type anharmonicity). In Fig. 8, we plot (a) the number of DBs and (b) the average energy of DBs as a function of the gamma-point mode amplitude at the time when L is maximal. It follows from the plots that N_{DB} again increases linearly with A nearly two times within the studied range of amplitudes, while E_{DB} increases with A very slowly.

Our main result is shown in Fig. 9, where the time-dependence of specific heat is plotted for the various mode amplitudes. From comparison of Fig. 6 and Fig. 9, it can be seen that the specific heat is maximal when the localization parameter is maximal. During the transition to thermal equilibrium, the specific heat decreases. From this, we conclude that the DBs increase the specific heat of the chain with soft-type anharmonicity.

V. PROPERTIES OF DISCRETE BREATHERS

Approximate solutions for DBs in the chain Eq. (3) have been derived in [104]. However, the solution reported for the hard-type anharmonicity cannot be used here because it is valid only for relatively wide DBs but in our simulations very sharp DBs are formed as the result of modulational instability, see Fig. 3. In the following we will give another approximate solution, which is valid for very sharp DBs in the case of hard-type anharmonicity. On the other hand, in the case of soft-type anharmonicity the emerging DBs are not very sharp, see Fig. 7, and the solution reported in [104] gives a reasonable accuracy.

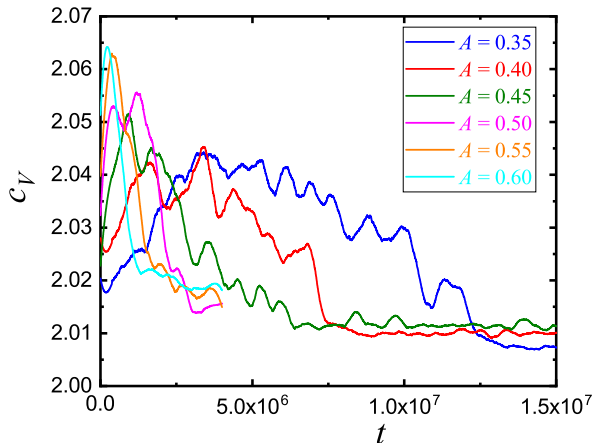


Figure 9: Localization parameter as the function of time for various amplitudes of the initially excited gamma-point mode. For all cases at $t = 0$ the localization parameter is $L = 1/N = 10^{-3}$. Modulational instability results in increase of L due to energy localization on DBs. Then L decreases because DBs gradually radiate energy and eventually system reaches thermal equilibrium with $L = 2 \times 10^{-3}$. Results for $\alpha = -1/24$ (soft-type anharmonicity).

Below we will reproduce that solution for the convenience of the reader.

A. Hard-type anharmonicity

For a very sharp DB localized on n -th particle, we assume that $u_{n-1} = u_{n+1} = 0$. Hence, Eq. (3) obtains the form

$$\ddot{u}_n + a_1 u_n + a_3 u_n^3 + a_5 u_n^5 = 0, \quad (12)$$

where

$$a_1 = \frac{2(s+k)}{m}, \quad a_3 = \frac{4\alpha}{m} \quad \text{and} \quad a_5 = \frac{6\beta}{m}.$$

The exact periodic solution to this equation has been reported, e.g., in [105] in the form

$$u_n = \frac{A_{DB} \text{cn}(P, M)}{\sqrt{\text{cn}^2(P, M) + \sqrt{\frac{6q_1}{q_2}} \text{sn}^2(P, M) \text{dn}^2(P, M)}}, \quad (13)$$

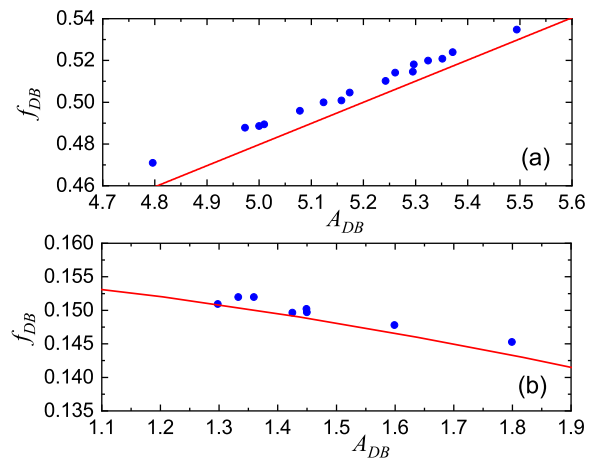


Figure 10: The DB Frequency (f_{DB}) as a function of the DB amplitude (A_{DB}), for (a) hard-type anharmonicity and (b) soft-type anharmonicity. The line in (a) is for the analytical solution Eq. (13), while the line in (b) for the solution Eq. (21). Scattered dots in (a) and (b) are for the chaotic breathers emerged as the result of modulational instability of the zone-boundary mode with the amplitude $A = 1.0$ and the Γ -point mode with $A = 0.6$, respectively.

where cn , sn and dn are the Jacobi elliptic functions, A_{DB} is the DB amplitude and

$$q_1 = a_1 + a_3 A_{DB}^2 + a_5 A_{DB}^4, \quad (14)$$

$$q_2 = 6a_1 + 3a_3 A_{DB}^2 + 2a_5 A_{DB}^4, \quad (15)$$

$$q_3 = 4a_1 + 3a_3 A_{DB}^2 + 2a_5 A_{DB}^4, \quad (16)$$

$$P = \left(\frac{q_1 q_2}{6} \right)^{\frac{1}{4}} t, \quad (17)$$

$$M = \frac{1}{2} - \frac{q_3}{4} \sqrt{\frac{3}{2q_1 q_2}}. \quad (18)$$

The solid line in Fig. 10(a) shows the relation between the DB frequency (f_{DB}) and the DB amplitude (A_{DB}) obtained from the analytical solution Eq. (13) to Eq. (12). Here we also plot the numerical results (scattered dots) for the DBs emerged in the simulations of the modulational instability of the zone-boundary mode with $A = 1.0$, see Fig. 3. It can be seen that the analytical solution is in a good agreement with the simulation results. The small difference (within 5%) between the numerical and analytical results can be attributed to the assumption, that the DB is localized on single particle, used in calculating the analytical solution. This assumption is responsible for underestimation of the rigidity of the actual breather. As the DB amplitude is increased, the degree of DB localization also increases and thus, the simulation results become closer to the analytical solution at higher amplitudes.

B. Soft-type anharmonicity

In the case of soft-type anharmonicity, for not very large displacements, Eq. (3) can be approximated by the Frenkel-Kontorova model [106]

$$m\ddot{u}_n = s(u_{n-1} - 2u_n + u_{n+1}) - \sin(u_n), \quad (19)$$

which reduces to the sine-Gordon equation in the continuum limit ($s \rightarrow \infty$),

$$u_{tt} - u_{xx} + \sin u = 0. \quad (20)$$

Then the well-known moving breather solution of Eq. (20) can be written in the discrete form to give an approximate solution to Eq. (19) as follows

$$u_n(t) = 4 \arctan \frac{\eta \cos[\zeta \omega_{\text{DB}}(t - v_{\text{DB}}n)]}{\omega_{\text{DB}} \cosh[\zeta \eta(n - v_{\text{DB}}t)]}, \quad (21)$$

where

$$\eta = \sqrt{1 - \omega_{\text{DB}}^2}, \quad \zeta = \frac{1}{\sqrt{1 - v_{\text{DB}}^2}}. \quad (22)$$

The solid line in Fig. 10(b) shows the relation between the DB frequency (f_{DB}) and the DB amplitude (A_{DB}) for soft-type anharmonicity obtained from the analytical solution Eq. (21). It is plotted against the numerical results (scattered dots) obtained from the simulation of modulational instability of the Γ -point mode with the amplitude $A = 0.6$. Again, the analytical solution is in good agreement with the simulation results (within 1%).

VI. CONCLUSIONS

In the present study, the effect of DBs on the specific heat of a nonlinear chain is discussed. Chaotic DBs arise in the chain as a result of modulational instability of particular extended vibrational modes, namely, the zone-boundary mode ($q = \pi$) for the case of hard-type anharmonicity and the Γ -point mode ($q = 0$) for the case of soft-type anharmonicity.

As it can be seen in Fig. 5, when DBs are excited in the chain with hard-type anharmonicity, the specific heat

is about 10% lower as compared to thermal equilibrium. For the soft-type anharmonicity (see Fig. 9), the specific heat reduces by about 2% during the transition from the regime with DBs to thermal equilibrium. This means that DBs reduce (increase) the heat capacity of the nonlinear chain with hard-type (soft-type) anharmonicity.

From this observation it follows that the heat capacity of the crystals having a gap in the phonon spectrum and supporting soft-type anharmonicity DBs (e.g., NaI [31, 32, 38–40], ordered alloys [51–54], and graphane [37]) should increase due to the excitation of DBs. For the crystals without a gap in the phonon spectrum (e.g., pure metals [45–50] and covalent crystals [43, 44]) only hard-type anharmonicity DBs can exist and their excitation will reduce heat capacity.

Note that in the experimental work [28] an increase of heat capacity of alpha-uranium at high temperatures was related to the contribution from DBs. Apparently this is a misleading interpretation since DBs in alpha-uranium are of the hard-type anharmonicity [48] and they can only *reduce* the heat capacity.

In future studies, it is planned to analyze the effect of DBs on other macroscopic properties of nonlinear chains and crystal lattices, e.g., on the elastic constants and thermal expansion. This work will suggest the way of indirect detection of DBs in crystals by measuring macroscopic properties sensitive to the presence of DBs.

Acknowledgments

The work of E.A.K. was supported by the Grant of the President of the Russian Federation for State support of young Russian scientists (No. MD-3639.2019.2). The work of D.X. is supported by NNSF (Grant No. 11575046) of China, NSF (Grant No. 2017J06002) of Fujian Province of China. The work of V.A.G. was supported by the MEPhI Academic Excellence Project (Contract No. 02.a03.21.0005, 27.08.2013). S.V.D. acknowledges the support of the Russian Foundation for Basic Research, Grant No. 19-02-00971. The work was partly supported by the Tomsk State University competitiveness improvement programme and State assignment of IMSP RAS.

-
- [1] A. S. Dolgov, *Sov. Phys. Solid State* **28**, 907 (1986).
 - [2] A. J. Sievers and S. Takeno, *Intrinsic Localized Modes in Anharmonic Crystals*, *Phys. Rev. Lett.* **61**, 970 (1988).
 - [3] J. B. Page, *Asymptotic solutions for localized vibrational modes in strongly anharmonic periodic systems*, *Phys. Rev. B* **41**, 7835 (1990).
 - [4] S. Flach and C. R. Willis, *Discrete breathers*, *Phys. Rep.* **295**, 181 (1998).
 - [5] S. Flach and A. V. Gorbach, *Discrete breathers — Advances in theory and applications*,

- Phys. Rep.* **467**, 1 (2008).
- [6] Y. Watanabe, T. Nishida, Y. Doi, and N. Sugimoto, *Experimental demonstration of excitation and propagation of intrinsic localized modes in a mass-spring chain*, *Phys. Lett. A* **382**, 1957 (2018).
- [7] J. Cuevas, L. Q. English, P. G. Kevrekidis, and M. Anderson, *Discrete Breathers in a Forced-Damped Array of Coupled Pendula: Modeling, Computation, and Experiment*, *Phys. Rev. Lett.* **102**, 224101 (2009).
- [8] F. M. Russell, Y. Zolotaryuk, J. C. Eilbeck, and

- T. Dauxois, Moving breathers in a chain of magnetic pendulums, *Phys. Rev. B* **55**, 6304 (1997).
- [9] K. Vorotnikov, Y. Starosvetsky, G. Theocharis, and P. G. Kevrekidis, Wave propagation in a strongly nonlinear locally resonant granular crystal, *Physica D* **365**, 27 (2018).
- [10] C. Chong, M. A. Porter, P. G. Kevrekidis, and C. Daraio, Nonlinear coherent structures in granular crystals, *J. Phys.: Condens. Matter* **29**, 413003 (2017).
- [11] Y. Zhang, D. M. McFarland, and A. F. Vakakis, Propagating discrete breathers in forced one-dimensional granular networks: theory and experiment, *Granular Matter* **19**, 59 (2017).
- [12] L. Liu, G. James, P. Kevrekidis, and A. Vainchtein, Strongly nonlinear waves in locally resonant granular chains, *Nonlinearity* **29**, 3496 (2016).
- [13] L. Liu, G. James, P. Kevrekidis, and A. Vainchtein, Breathers in a locally resonant granular chain with pre-compression, *Physica D* **331**, 27 (2016).
- [14] K. R. Jayaprakash, Y. Starosvetsky, A. F. Vakakis, M. Peeters, and G. Kerschen, Nonlinear normal modes and band zones in granular chains with no pre-compression, *Nonlinear Dynam.* **63**, 359 (2011).
- [15] G. Theocharis, N. Boechler, P. G. Kevrekidis, S. Job, M. A. Porter, and C. Daraio, Intrinsic energy localization through discrete gap breathers in one-dimensional diatomic granular crystals, *Phys. Rev. E* **82**, 056604 (2010).
- [16] N. Boechler, G. Theocharis, S. Job, P. G. Kevrekidis, M. A. Porter, and C. Daraio, Discrete Breathers in One-Dimensional Diatomic Granular Crystals, *Phys. Rev. Lett.* **104**, 244302 (2010).
- [17] M. Sato, B. E. Hubbard, and A. J. Sievers, Nonlinear energy localization and its manipulation in micromechanical oscillator arrays, *Rev. Mod. Phys.* **78**, 137 (2006).
- [18] M. Sato, B. E. Hubbard, A. J. Sievers, B. Ilic, and H. G. Craighead, Optical manipulation of intrinsic localized vibrational energy in cantilever arrays, *Europhys. Lett.* **66**, 318 (2004).
- [19] M. Sato, B. E. Hubbard, A. J. Sievers, B. Ilic, D. A. Czaplewski, and H. G. Craighead, Observation of Locked Intrinsic Localized Vibrational Modes in a Micromechanical Oscillator Array, *Phys. Rev. Lett.* **90**, 044102 (2003).
- [20] F. Palmero, L. Q. English, X.-L. Chen, W. Li, J. Cuevas-Maraver, and P. G. Kevrekidis, Experimental and numerical observation of dark and bright breathers in the band gap of a diatomic electrical lattice, *Phys. Rev. E* **99**, 032206 (2019).
- [21] A. Gomez-Rojas and P. Halevi, Discrete breathers in an electric lattice with an impurity: Birth, interaction, and death, *Phys. Rev. E* **97**, 022225 (2018).
- [22] R. Stearrett and L. Q. English, Experimental generation of intrinsic localized modes in a discrete electrical transmission line, *J. Phys. D: Appl. Phys.* **40**, 5394 (2007).
- [23] F. Lederer, G. I. Stegeman, D. N. Christodoulides, G. Assanto, M. Segev, and Y. Silberberg, Discrete solitons in optics, *Phys. Rep.* **463**, 1 (2008).
- [24] E. Trias, J. J. Mazo, and T. P. Orlando, Discrete Breathers in Nonlinear Lattices: Experimental Detection in a Josephson Array, *Phys. Rev. Lett.* **84**, 741 (2000).
- [25] P. Binder, D. Abraimov, A. V. Ustinov, S. Flach, and Y. Zolotaryuk, Observation of Breathers in Josephson Ladders, *Phys. Rev. Lett.* **84**, 745 (2000).
- [26] S. V. Dmitriev, E. A. Korznikova, J. A. Baimova, and M. G. Velarde, Discrete breathers in crystals, *Phys. Usp.* **59**, 446 (2016).
- [27] M. E. Manley *et al.*, Intrinsically localized vibrations and the mechanical properties of α -uranium, *J. Alloys Compd.* **444**, 129 (2007).
- [28] B. Mihaila *et al.*, Pinning Frequencies of the Collective Modes in α -Uranium, *Phys. Rev. Lett.* **96**, 076401 (2006).
- [29] M.E. Manley *et al.*, Formation of a New Dynamical Mode in α -Uranium Observed by Inelastic X-Ray and Neutron Scattering, *Phys. Rev. Lett.* **96**, 125501 (2006).
- [30] T. Markovich, E. Polturak, J. Bossy, and E. Farhi, Observation of a New Excitation in bcc ^4He by Inelastic Neutron Scattering, *Phys. Rev. Lett.* **88**, 195301 (2002).
- [31] M. E. Manley *et al.*, Intrinsic localized modes observed in the high-temperature vibrational spectrum of NaI, *Phys. Rev. B* **79**, 134304 (2009).
- [32] M. E. Manley, D. L. Abernathy, N. I. Agladze, and A. J. Sievers, Symmetry-breaking dynamical pattern and localization observed in the equilibrium vibrational spectrum of NaI, *Sci. Rep.* **1**, 4 (2011).
- [33] W. Liang, G. M. Vanacore, and A. H. Zewail, Observing (non)linear lattice dynamics in graphite by ultrafast Kikuchi diffraction, *Proc. Natl. Acad. Sci. USA* **111**, 5491 (2014).
- [34] M. E. Manley *et al.*, Intrinsic anharmonic localization in thermoelectric PbSe, *Nature Commun.* **10**, 1928 (2019).
- [35] A. J. Sievers, M. Sato, J. B. Page, and T. Rössler, Thermally populated intrinsic localized modes in pure alkali halide crystals, *Phys. Rev. B* **88**, 104305 (2013).
- [36] I. P. Lobzenko, G. M. Chechin, G. S. Bezuglova, Yu. A. Baimova, E. A. Korznikova, and S. V. Dmitriev, Ab initio simulation of gap discrete breathers in strained graphene, *Phys. Solid State* **58**, 633 (2016).
- [37] G. M. Chechin, S. V. Dmitriev, I. P. Lobzenko, and D. S. Ryabov, Properties of discrete breathers in graphene from *ab initio* simulations, *Phys. Rev. B* **90**, 045432 (2014).
- [38] S. A. Kiselev and A. J. Sievers, Generation of intrinsic vibrational gap modes in three-dimensional ionic crystals, *Phys. Rev. B* **55**, 5755 (1997).
- [39] L. Z. Khadeeva and S. V. Dmitriev, Discrete breathers in crystals with NaCl structure, *Phys. Rev. B* **81**, 214306 (2010).
- [40] A. Riviere, S. Lepri, D. Colognesi, and F. Piazza, Wavelet imaging of transient energy localization in nonlinear systems at thermal equilibrium: The case study of NaI crystals at high temperature, *Phys. Rev. B* **99**, 024307 (2019).
- [41] A. A. Kistanov, R. T. Murzaev, S. V. Dmitriev, V. I. Dubinko, and V. V. Khizhnyakov, Moving discrete breathers in a monoatomic two-dimensional crystal, *JETP Lett.* **99**, 353 (2014).
- [42] E. A. Korznikova, S. Yu. Fomin, E. G. Soboleva, and S. V. Dmitriev, Highly symmetric discrete breather in a two-dimensional Morse crystal, *JETP Lett.* **103**, 277 (2016).
- [43] N. K. Voulgarakis, G. Hadjisavvas, P. C. Keilires, and G. P. Tsironis, Computational inves-

- tigation of intrinsic localization in crystalline Si, Phys. Rev. B **69**, 113201 (2004).
- [44] R. T. Murzaev, D. V. Bachurina, E. A. Korznikova, and S. V. Dmitriev, Localized vibrational modes in diamond, Phys. Lett. A **381**, 1003 (2017).
- [45] M. Haas, V. Hizhnyakov, A. Shelkan, M. Klopov, and A. J. Sievers, Prediction of high-frequency intrinsic localized modes in Ni and Nb, Phys. Rev. B **84**, 144303 (2011).
- [46] O. V. Bachurina, Linear discrete breather in fcc metals, Comp. Mater. Sci. **160**, 217 (2019).
- [47] O. V. Bachurina, R. T. Murzaev, A. S. Semenov, E. A. Korznikova, and S. V. Dmitriev, Properties of Moving Discrete Breathers in Beryllium, Phys. Solid State **60**, 989 (2018).
- [48] R. T. Murzaev, R. I. Babicheva, K. Zhou, E. A. Korznikova, S. Y. Fomin, V. I. Dubinko, and S. V. Dmitriev, Discrete breathers in alpha-uranium, Eur. Phys. J. B **89**, 168 (2016).
- [49] R. T. Murzaev, A. A. Kistanov, V. I. Dubinko, D. A. Terentyev, and S. V. Dmitriev, Moving discrete breathers in bcc metals V, Fe and W, Comp. Mater. Sci. **98**, 88 (2015).
- [50] D. A. Terentyev, A. V. Dubinko, V. I. Dubinko, S. V. Dmitriev, E. E. Zhurkin, and M. V. Sorokin, Interaction of discrete breathers with primary lattice defects in bcc Fe, Model. Simul. Mater. Sc. **23**, 085007 (2015).
- [51] V. Dubinko, D. Laptev, D. Terentyev, S. V. Dmitriev, and K. Irwin, Assessment of discrete breathers in the metallic hydrides, Comp. Mater. Sci. **158**, 389 (2019).
- [52] P. V. Zakharov, E. A. Korznikova, S. V. Dmitriev, E. G. Ekomasov, and K. Zhou, Surface discrete breathers in Pt_3Al intermetallic alloy, Surf. Sci. **679**, 1 (2019).
- [53] M. D. Starostenkov, A. I. Potekaev, S. V. Dmitriev, P. V. Zakharov, A. M. Eremin, and V. V. Kulagina, Dynamics of Discrete Breathers in a Pt_3Al Crystal, Russ. Phys. J. **58**, 1353 (2016).
- [54] N. N. Medvedev, M. D. Starostenkov, and M. E. Manley, Energy localization on the Al sublattice of Pt_3Al with $L1_2$ order, J. Appl. Phys. **114**, 213506 (2013).
- [55] J. A. Baimova, E. A. Korznikova, I. P. Lobzenko, and S. V. Dmitriev, Discrete breathers in carbon and hydrocarbon nanostructures, Rev. Adv. Mater. Sci. **42**, 68 (2015).
- [56] B. Liu, J. A. Baimova, S. V. Dmitriev, X. Wang, H. Zhu, and K. Zhou, Discrete breathers in hydrogenated graphene, J. Phys. D: Appl. Phys. **46**, 305302 (2013).
- [57] E. A. Korznikova, J. A. Baimova, and S. V. Dmitriev, Effect of strain on gap discrete breathers at the edge of armchair graphene nanoribbons, Europhys. Lett. **102**, 60004 (2013).
- [58] J. A. Baimova, S. V. Dmitriev, and K. Zhou, Discrete breather clusters in strained graphene, Europhys. Lett. **100**, 36005 (2012).
- [59] E. A. Korznikova, A. V. Savin, Yu. A. Baimova, S. V. Dmitriev, and R. R. Mulyukov, Discrete breather on the edge of the graphene sheet with the armchair orientation, JETP Lett. **96**, 222 (2012).
- [60] A. V. Savin and Yu. S. Kivshar, Nonlinear breatherlike localized modes in C_{60} nanocrystals, Phys. Rev. B **85**, 125427 (2012).
- [61] Y. Yamayose, Y. Kinoshita, Y. Doi, A. Nakatani, and T. Kitamura, Excitation of intrinsic localized modes in a graphene sheet, Europhys. Lett. **80**, 40008 (2007).
- [62] T. Shimada, D. Shirasaki, and T. Kitamura, Stone-Wales transformations triggered by intrinsic localized modes in carbon nanotubes, Phys. Rev. B **81**, 035401 (2010).
- [63] Y. Kinoshita, Y. Yamayose, Y. Doi, A. Nakatani, and T. Kitamura, Selective excitations of intrinsic localized modes of atomic scales in carbon nanotubes, Phys. Rev. B **77**, 024307 (2008).
- [64] Y. Doi and A. Nakatani, Numerical Study on Unstable Perturbation of Intrinsic Localized Modes in Graphene, J. Solid Mech. Mater. Eng. **6**, 71 (2012).
- [65] L. Z. Khadeeva, S. V. Dmitriev, and Yu. S. Kivshar, Discrete breathers in deformed graphene, JETP Lett. **94**, 539 (2011).
- [66] E. Barani, I. P. Lobzenko, E. A. Korznikova, E. G. Soboleva, S. V. Dmitriev, K. Zhou, and A. M. Marjaneh, Transverse discrete breathers in unstrained graphene Eur. Phys. J. B, **90**, 38 (2017).
- [67] I. Evazzade, I. P. Lobzenko, E. A. Korznikova, I. A. Ovid'Ko, M. R. Roknabadi, and S. V. Dmitriev, Energy transfer in strained graphene assisted by discrete breathers excited by external ac driving, Phys. Rev. B **95**, 035423 (2017).
- [68] E. Barani, E. A. Korznikova, A. P. Chetverikov, K. Zhou, and S. V. Dmitriev, Gap discrete breathers in strained boron nitride, Phys. Lett. A **381**, 3553 (2017).
- [69] A. P. Chetverikov, K. S. Sergeev, and V. D. Lakhno, Trapping and transport of charges in DNA by mobile discrete breathers, Math. Biol. Bioinf. **13**, t59 (2018).
- [70] F. Piazza and Y.-H. Sanejouand, Discrete breathers in protein structures, Phys. Biol. **5**, 026001 (2008).
- [71] B. Juanico, Y.-H. Sanejouand, F. Piazza, and P. De Los Rios, Discrete Breathers in Nonlinear Network Models of Proteins, Phys. Rev. Lett. **99**, 238104 (2007).
- [72] M. Peyrard, S. Cuesta-López, and G. James, Nonlinear Analysis of the Dynamics of DNA Breathing, J. Biol. Phys. **35**, 73 (2009).
- [73] M. E. Manley, Impact of intrinsic localized modes of atomic motion on materials properties, Acta Mater. **58**, 2926 (2010).
- [74] Y. Ming, D.-B. Ling, H.-M. Li, and Z.-J. Ding, Energy thresholds of discrete breathers in thermal equilibrium and relaxation processes, Chaos **27**, 063106 (2017).
- [75] D. Xiong, D. Saadatmand, and S. V. Dmitriev, Crossover from ballistic to normal heat transport in the ϕ^4 lattice: If nonconservation of momentum is the reason, what is the mechanism?, Phys. Rev. E **96**, 042109 (2017).
- [76] L. Z. Khadeeva and S. V. Dmitriev, Lifetime of gap discrete breathers in diatomic crystals at thermal equilibrium, Phys. Rev. B **84**, 144304 (2011).
- [77] A. A. Kistanov and S. V. Dmitriev, Spontaneous excitation of discrete breathers in crystals with the NaCl structure at elevated temperatures, Phys. Solid State **54**, 1648 (2012).
- [78] M. V. Ivanchenko, O. I. Kanakov, V. D. Shalfeev, and S. Flach, Discrete breathers in transient processes and thermal equilibrium, Physica D **198**, 120 (2004).
- [79] M. Eleftheriou and S. Flach, Discrete breathers in thermal equilibrium: distributions and energy gaps, Physica D **202**, 142 (2005).
- [80] B. Gershgorin, Yu. V. Lvov, and D. Cai, Renormalized Waves and Discrete Breathers in β -Fermi-Pasta-Ulam

- Chains, *Phys. Rev. Lett.* **95**, 264302 (2005).
- [81] M. Eleftheriou, S. Flach, and G. P. Tsironis, Breathers in one-dimensional nonlinear thermalized lattice with an energy gap, *Physica D* **186**, 20 (2003).
- [82] G. P. Tsironis and S. Aubry, Slow Relaxation Phenomena Induced by Breathers in Nonlinear Lattices, *Phys. Rev. Lett.* **77**, 5225 (1996).
- [83] R. Reigada, A. Sarmiento, and K. Lindenberg, Asymptotic dynamics of breathers in Fermi-Pasta-Ulam chains, *Phys. Rev. E* **66**, 046607 (2002).
- [84] A. Bikaki, N. K. Voulgarakis, S. Aubry, and G. P. Tsironis, Energy relaxation in discrete nonlinear lattices, *Phys. Rev. E* **59**, 1234 (1999).
- [85] F. Piazza, S. Lepri, and R. Livi, Cooling nonlinear lattices toward energy localization, *Chaos* **13**, 637 (2003).
- [86] M. Eleftheriou, S. Lepri, R. Livi, and F. Piazza, Stretched-exponential relaxation in arrays of coupled rotators, *Physica D* **204**, 230 (2005).
- [87] F. Piazza, S. Lepri, and R. Livi, Slow energy relaxation and localization in 1D lattices, *J. Phys. A: Math. Gen.* **34**, 9803 (2001).
- [88] F. Piazza, P. De Los Rios, and Y.-H. Sanejouand, Slow Energy Relaxation of Macromolecules and Nanoclusters in Solution, *Phys. Rev. Lett.* **94**, 145502 (2005).
- [89] B. Juanico, Y.-H. Sanejouand, F. Piazza, and P. De Los Rios, Discrete Breathers in Nonlinear Network Models of Proteins, *Phys. Rev. Lett.* **99**, 238104 (2007).
- [90] R. Reigada, A. Sarmiento, and K. Lindenberg, Energy relaxation in nonlinear one-dimensional lattices, *Phys. Rev. E* **64**, 066608 (2001).
- [91] R. Reigada, A. Sarmiento, and K. Lindenberg, Energy relaxation in Fermi-Pasta-Ulam arrays, *Physica A* **305**, 467 (2002).
- [92] R. Reigada, A. Sarmiento, and K. Lindenberg, Breathers and thermal relaxation in Fermi-Pasta-Ulam arrays, *Chaos* **13**, 646 (2003).
- [93] G. P. Tsironis, A. R. Bishop, A. V. Savin, and A. V. Zolotaryuk, Dependence of thermal conductivity on discrete breathers in lattices, *Phys. Rev. E* **60**, 6610 (1999).
- [94] V. M. Burlakov and S. Kiselev, Molecular-dynamics simulation of the decay kinetics of uniform excitation of an anharmonic 1D chain, *Sov. Phys. JETP* **72**, 854 (1991).
- [95] V. V. Mirnov, A. J. Lichtenberg, and H. Guclu, Chaotic breather formation, coalescence, and evolution to energy equipartition in an oscillatory chain, *Physica D* **157**, 251 (2001).
- [96] K. Ullmann, A. J. Lichtenberg, and G. Corso, Energy equipartition starting from high-frequency modes in the Fermi-Pasta-Ulam β oscillator chain, *Phys. Rev. E* **61**, 2471 (2000).
- [97] Yu. A. Kosevich and S. Lepri, Modulational instability and energy localization in anharmonic lattices at finite energy density, *Phys. Rev. B* **61**, 299 (2000).
- [98] T. Cretegny, T. Dauxois, S. Ruffo, and A. Torcini, Localization and equipartition of energy in the β -FPU chain: Chaotic breathers, *Physica D* **121**, 109 (1998).
- [99] B. Tang and K. Deng, Discrete breathers and modulational instability in a discrete ϕ^4 nonlinear lattice with next-nearest-neighbor couplings, *Nonlinear Dyn.* **88**, 2417 (2017).
- [100] E. A. Korznikova, D. V. Bachurin, S. Yu. Fomin, A. P. Chetverikov, and S. V. Dmitriev, Instability of vibrational modes in hexagonal lattice, *Eur. Phys. J. B* **90**, 23 (2017).
- [101] L. Kavitha, A. Mohamadou, E. Parasuraman, D. Gopi, N. Akila, and A. Prabhu, Modulational instability and nano-scale energy localization in ferromagnetic spin chain with higher order dispersive interactions, *J. Magn. Magn. Mat.* **404**, 91 (2016).
- [102] L. Kavitha, E. Parasuraman, D. Gopi, A. Prabhu, and R. A. Vicencio, Nonlinear nano-scale localized breather modes in a discrete weak ferromagnetic spin lattice, *J. Magn. Magn. Mat.* **401**, 394 (2016).
- [103] K. Ikeda, Y. Doi, B. F. Feng, and T. Kawahara, Chaotic breathers of two types in a two-dimensional Morse lattice with an on-site harmonic potential, *Physica D* **225**, 184 (2007).
- [104] D. Saadatmand, D. Xiong, V. A. Kuzkin, A. M. Krivtsov, A. V. Savin, and S. V. Dmitriev, Discrete breathers assist energy transfer to ac-driven nonlinear chains, *Phys. Rev. E* **97**, 022217 (2018).
- [105] A. Beléndez, T. Beléndez, F. J. Martínez, C. Pascual, M. L. Alvarez, and E. Arribas, Exact solution for the unforced Duffing oscillator with cubic and quintic nonlinearities, *Nonlinear Dyn.* **86**, 1687 (2016).
- [106] O. M. Braun and Yu. S. Kivshar, Nonlinear dynamics of the Frenkel-Kontorova model, *Phys. Rep.* **306**, 1 (1998).